



XXVIIIth International Conference on Ultrarelativistic Nucleus-Nucleus Collisions
(Quark Matter 2019)

“QM19 summary talk”:
Outlook and future of heavy-ion collisions

Constantin Loizides

ORNL, Oak Ridge, USA

Abstract

A summary of the QM19 conference is given by highlighting a few selected results. These are discussed as examples to illustrate the exciting future of heavy-ion collisions and the need for further instrumentation. (The arXiv version is significantly longer than the printed proceedings, with more figures.)

1. Introduction

The goal of heavy-ion physics [1] is to understand the phase diagram of Quantum Chromo Dynamics (QCD) as a function of the temperature (T) and baryon chemical potential (μ_B), as shown in Fig. 1. At high temperature and/or high baryon chemical a transition occurs, from ordinary matter, where the hadronic degrees of freedom are dominant, to a Quark Gluon Plasma (QGP), where the dominant degrees of freedom are quark and gluons, which in ordinary matter are confined into hadrons. Lattice QCD calculations [2] predict the presence of a Critical Endpoint (CE) somewhere in the region $T < 140, \mu_B > 300$ MeV with a first-order phase transition at higher μ_B and a cross-over transition at $T \approx 155$ MeV and lower μ_B . Immense experimental and theoretical effort is underway to characterize and understand the phase structure of QCD, and the emergence of collectivity and matter properties, and the underlying equation of state (EoS) from first principles. Following the presentation at the conference [3], these proceedings are structured into the following topics:

- the high-density frontier (Sec. 2) to study the onset of deconfinement, to search for the CE and the first-order phase transition, and at very high μ_B to provide constraints for the neutron star structure and its EoS;
- the high-energy frontier (Sec. 3) to quantify the fluid properties of QGP and to relate them to its microscopic structure;
- the cold nuclear matter or small- x frontier (Sec. 4) to characterize properties of cold nuclear matter, and understand the structure of protons and nuclei at small Bjorken- x ;

arXiv:2007.00710v1 [nucl-ex] 1 Jul 2020

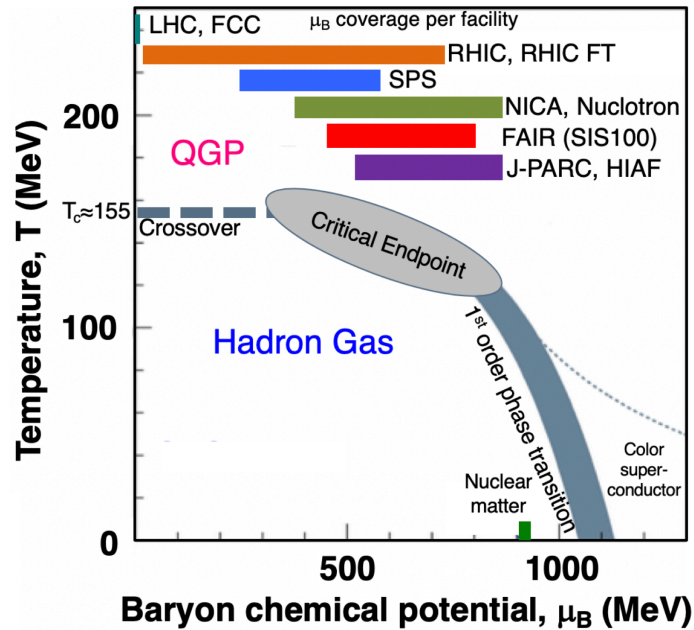


Fig. 1. The QCD phase diagram versus temperature and bayon chemical potential. Indicated are the nuclear matter, hadron gas and QGP phases, as well as the approximate region for the Critical Endpoint, and the first-order and cross-over phase transitions. Current and future facilities probing different region in μ_B are: LHC [4], FCC [5], RHIC [6], and the RHIC fixed-target program [7], SPS [8, 9], NICA [10], FAIR [11] and J-PARC [12]. Figure from [13].

- the ultra-precision near and far future (Sec. 5) with the planned Electron Ion Collider (EIC) and the proposed new future experimental equipment at the Large Hadron Collider (LHC) and beyond.

2. The high-density frontier

Predictions for the existence and exact location of the CE at finite μ_B have been continuously improved over the past years. New lattice QCD results from the WB collaboration [14] using the imaginary μ_B method are consistent with previous calculations by the HotQCD collaboration, but have much smaller uncertainty, and hence add further evidence that the location of CP is disfavoured for $\mu_B < 300$ MeV. Where possible, lattice QCD predictions were already confronted with experimental data [15]. The experimental approach [16] is to probe different regions of the QCD matter phase diagram by extracting the freeze-out parameters (T , μ_B) from statistical model fits to hadron yields measured at LHC (few TeV) down to SIS18 (few GeV) collision energies. In this way, the vicinity of the phase boundary will be explored from $T \approx 155$ and $\mu_B \approx 0$ MeV down to about $T = 80$ and $\mu_B = 900$ MeV as shown in Fig. 1.

The CE is characterized as a divergence in the correlation length of the underlying system, and hence manifests as a divergence of the associated susceptibilities. Experimentally, ratios of susceptibilities are accessible through event-by-event fluctuations in conserved quantities, such as electric charge or baryon number. In particular, higher-order moments of net-proton distributions, which are a proxy for baryon number, are expected to be sensitive to the CE. First results of C_6/C_2 of net-proton distributions were reported [17], which for central AuAu collisions at $\sqrt{s_{NN}} = 200$ GeV are negative, as expected from lattice QCD, while they were found to be positive for central AuAu collisions at $\sqrt{s_{NN}} = 54.4$ GeV. Albeit being only a 2σ -effect at present, the result may indicate the expected $O(4)$ criticality in the cross-over region [18]. Furthermore, a crucial study was performed [19] by checking that the freeze-out parameters deduced from mean hadron yields agree with those from grand-canonical fluctuations of conserved quantities for central collisions. This demonstrates for the first time, using fluctuation observables, that a femto-scale system

attains thermalization. A low $\sqrt{s_{NN}}$ (< 19.6 GeV) the presented study however indicates that the created system may be too dilute to reach equilibrium or exhibits different relaxation times for different moments. In view of the search for the CE this should be followed-up on.

A first-order phase transition is characterized by an unstable co-existence (spinodal) region corresponding to a softest point in the EoS. Direct flow (v_1) which is sensitive to the compressibility of the created matter, is hence a key observable in the beam energy scan (BES) program. The slope of the rapidity-odd component at mid-rapidity was reported as a function of beam energy for various identified mesons and baryons [20]. Mesons and anti-baryons exhibit negative slope over the whole range of beam energies, while baryons (p, Λ) exhibit a change of slope around 14.5 GeV. In hydrodynamical models a change of slope implies a minimum in v_1 , and hence was proposed as a signature of a first-order phase transition [21]. However, to consistently treat effects from spectator matter and baryon stopping, calculations in the frame of the BEST collaboration [22] would be needed using more realistic 3D hydrodynamic calculations at finite μ_B [23], with an EoS with and without CE [24]. First data from the STAR fixed-target (FT) program, the v_1 of the ϕ -meson at $\sqrt{s_{NN}} = 4.5$ GeV were also shown, but the statistical uncertainties are too large to allow for additional conclusions. More results, from BES phase 2, and the fixed-target program, are eagerly awaited.

3. The high-energy frontier

The high-energy experiments at RHIC and LHC continue to produce data with ever increasing precision in measuring bulk properties. At the conference, for example, new results of longitudinal flow decorrelations at LHC [25] and their energy dependence at RHIC [26], linear and non-linear flow modes [27] and higher order cumulant elliptic flow and fluctuations [28] of identified particles in PbPb collisions at $\sqrt{s_{NN}} = 5.02$ TeV were presented. These and many more data are now rigorously used in Bayesian extraction of bulk properties, for example using the JETSCAPE framework [29]. It was argued [30] that RHIC and LHC data add complementary constraints, and that there are non-negligible uncertainties in the transition from fluid cells to particles (viscous corrections). In developing community frameworks like JETSCAPE, it is important to highlight and maintain the “plug-and-play” approach of the framework, which allows one to interchange and study different descriptions of the various stages of the collision. Furthermore, we need to insist that contributing authors release their pieces of code as open source promptly.

The precision reached in the J/ψ nuclear modification factor at mid-rapidity from ALICE [31] is now good enough to clearly see predicted behavior of the R_{AA} from statistical hadronization or regeneration [32–34] counteracting Debye screening: A clear minimum is observed in peripheral collisions ($N_{part} \sim 100$), beyond which the R_{AA} rises for more central collisions almost reaching unity in central collisions. Consequently, one also observes large flow as well as triangular flow due to “approximately thermalized” charm at low p_T [35]. The total charm cross section needs to be measured, since it is the natural normalization for J/ψ measurements. Knowing it precisely allows one to reduce model uncertainties by constraining shadowing effects, and set precise limits on the expected R_{AA} . Unity is not a priori a limiting value; the J/ψ R_{AA} can be larger than one [16] With a “brute-force” combinatorial extraction of D meson production down to 0.5 GeV/c, first constraints of the total charm cross section in PbPb were placed [36]. Better performance and more statistics will be expected in Run-3 after the LS2 ALICE upgrades.

The situation for the Y is different as due to its much heavier mass one does not expect a significant regeneration component. Broadening of its spectral widths on the lattice for finite temperature, presented at the conference [37], is compatible with the sequential dissociation picture. Sequential dissociation is clearly established for the Y family, and observed to be significantly stronger in PbPb than pPb collisions [38]. In pPb collisions, the suppression usually is attributed to comoving nuclear matter, but could in principle also be partially from the onset of screening. Elliptic flow was found to be consistent with zero [39, 40], however from extrapolating Blast Wave fits of existing data, one expects significant v_2 only for $p_T > 10$ GeV [41].

Understanding and characterizing parton energy loss continues to evolve from rather qualitative to more-and-more sophisticated and precise level. A milestone was reached with the first measurement of the jet fragmentation of jets recoiling of an isolated photon [42]. The data clearly exhibit the expected “text book” result that soft (low- z) particles are enhanced, while hard (high- z) are suppressed, as predicted since more

than 20 years (e.g. see [43] and references therein). Detailed measurements using isolated photon–jet correlations will play a key role to precisely quantify jet modification in Run-3/4 at the LHC¹ and in the sPHENIX era at RHIC. Measurements of inclusive jet R_{AA} were performed from about 50 to 500 GeV/ c for $R = 0.4$ in PbPb collisions at $\sqrt{s_{NN}} = 5.02$ TeV, and rather good agreement was found between data and models [45, 46]. It was hence surprising that the predictions [47] for larger radii and to higher p_T vary considerably indicating that the limited available measurements in the past year attracted the calculations. In order to avoid tuning of models to specific results, we could define a set of reference measurements (accord) that every jet model has to be able to describe before one trusts its prediction for a different observable. The CMS collaboration released new results [47] of R_{AA} for high energy jets up to $R = 1.0$, which yield $R_{AA} \approx 0.8$ above 300 GeV/ c for central PbPb collisions at $\sqrt{s_{NN}} = 5.02$ TeV. Peripheral collisions are consistent with unity, in particular when taking into account also the presence of the centrality bias [48]. The jet suppression for large radii in central collisions is similar to that of charged particles at ~ 200 GeV/ c [49], indicating the sought-after consistency between inclusive charged particle and jet R_{AA} at high p_T and large enough radius. Still, with new data from Run-3/4, it is important to measure both to even higher p_T , to reduce uncertainties, and to investigate if $R_{AA} \sim 1$ will be reached. Further progress with jet measurements to lower p_T and large radii (≥ 0.4) can be made by using Machine Learning methods trained on properties of the jet constituents in pp collisions [50]. First results have already been presented [51], and confirm the previously established picture of strong quenching at low jet p_T . However, in particular for large jet radii of $R = 0.6$ a potential bias induced by changed jet fragmentation needs to be investigated.

Substructure and reclustering techniques are extremely promising window to access the partonic structure of the shower [52]. New evidence for the coherent/wide angle energy loss picture have been presented at the conference. Symmetric splittings for wide-angles were reported to be suppressed relative to vacuum [53] and single sub-jets less exhibit less suppression than jets with multiple subjets [54].

One of the frontiers of the high-energy program is to study the evolution and onset of QGP phenomena in smaller collision systems like pA and pp collisions [55]. The yields of strange and multi-strange particles (relative to pions) increase smoothly with multiplicity, rather independent of collision species and energy [56] reaching a value predicted by statistical models in central PbPb collisions. The increase with multiplicity in smaller systems can be regarded as lifting of canonical suppression [57]. The rapid rise at low multiplicity plus the presence of many QGP signatures in pp and pPb collisions [58] lead to the development of “core/corona” models. In these models, the core “hydrodynamizes”, while the corona does not and instead is treated as a superposition of independent nucleon–nucleon collision. In this way, good description of data across all systems is achieved with a rather universal approach (similar to EPOS) [59].

The observed enhancement in the strange particle yields versus multiplicity result from the fact that there is a pedestal effect: The strange particle yields depend approximately linearly on multiplicity but only above some minimum multiplicity (threshold), while the pion yields do not exhibit any apparent threshold. Hence, normalizing the strange particle yields with the pion yields creates an enhancement $\propto (1 - M_0/M)$, which leads to a rise with M that is most apparent at low multiplicities. In microscopic models one can interpret the observed threshold in several ways: i) The yield increases with the number of overlapping strings, i.e. as a multi-string effect related to the string density driving the increase of strangeness production that however quickly saturates at higher multiplicity. ii) There is minimum associated multiplicity necessary for multi-strange particle production and/or different scaling of soft and (semi-)hard processes, i.e. a single string effect leading to suppression at low multiplicity that is reduced at higher multiplicity. To further probe production mechanism of strangeness can be achieved by measuring two-particle angular correlations (associated production) between same and opposite sign strange and non-strange particles [60]. These studies in particular when they involve also the Ω baryon will greatly benefit from the large increase in statistics of the 200/pb pp program planned for Run-3/4 [61].

The Λ_c^+/D ratio versus multiplicity at mid-rapidity measured in several p_T -ranges for pp, pPb and PbPb collisions at $\sqrt{s_{NN}} = 5.02$ TeV [36] shown in Fig. 2 exhibits surprising features: The ratios, in particular for lower p_T , smoothly increase with multiplicity from low multiplicity pp to central PbPb collisions. At

¹At LHC also Z-jet correlations are becoming available [44]

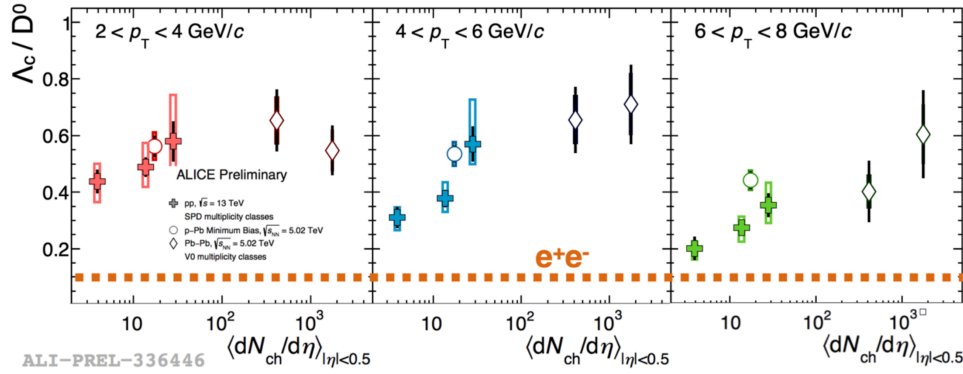


Fig. 2. The Λ_c^+ / D ratio versus multiplicity at mid-rapidity measured in several p_T -ranges for pp, pPb and PbPb collisions at $\sqrt{s_{NN}} = 5.02$ TeV compared to e^+e^- collisions [36].

the lowest measured multiplicity interval (below the pp average) the ratio at $2 < p_T < 4$ GeV/c is already significant (4 times) larger than that measured in e^+e^- collisions, while for the highest multiplicity interval it approaches the value seen in central PbPb collisions. The result is in qualitative agreement with the “recombination” hypothesis saturating already few (~ 6) times the average pp multiplicity, which requires the presence of a local space-time density. Alternative mechanisms like implemented in PYTHIA (“color reconnection”) can describe the data (but are not universal). The new data open up research on hadronization in pp collisions and future ep (eA) colliders.

In pp collisions at 13 TeV, heavier particles up to D-mesons exhibit finite $v_2 > 0$, while $v_2 \approx 0$ for B-mesons [62, 63]. Unlike at RHIC, where the geometry of the initial state can be engineered through the collisions of proton, deuteron or helium on gold [64], at LHC the dependence on geometry can only be more indirectly probed. Still, measurements of v_2 in Z-tagged pp events (which lead to more “central” events), and in photo-nuclear reactions (which can be regarded as a ρ -nucleus collision), reveal finite $v_2 > 0$ [65, 66], while $v_2 \approx 0$ was found in ee or ep collisions [67, 68]. In particular, for those systems where $v_2 \approx 0$, it would be good to follow up with other measurements like identified particle p_T spectra, mean p_T , or yield ratios versus p_T to check for absence of collectivity in observables related to v_2 . New calculations for small systems, where initial and final state effects were consistently treated, suggest the dominance of the final state effects beyond $dN/d\eta > 10$ [69]. Together with the large set of observables, which in PbPb collisions undoubtedly would be interpreted as QGP signals, this makes it plausible that we indeed observe the sQGP even down to multiplicities just above that of minbias pp collisions at LHC energies. While in 2015, there was a large debate whether it is possible [58], we should now focus on understanding how it is realized in QCD and what it implies.

Although the presence of flow without observable jet quenching does not rule out having a “mini” QGP, one of the key questions is the apparent absence of parton energy loss in small systems. Above a few GeV/c, nuclear modification factors measured in minimum bias pA collisions at mid-rapidity are consistent with pQCD calculations including nuclear PDFs (see references in [58]). Observing a suppression directly in light-particle flavor spectra is complicated due to the selection bias introduced by the “event-activity categorization” [70]. At high $p_T > 10$ GeV/c, v_2 is understood to reflect the path-length dependence of parton energy loss in PbPb collisions [71]. Therefore, the new data from ATLAS [72], which demonstrated significant non-zero v_2 values up to high $p_T \sim 50$ GeV/c in pPb collisions measured using the template fit method, are puzzling. They can not be consistently interpreted as due to parton energy loss, since the latter would imply R_{pPb} to be significantly below unity, not seen in data. Furthermore, the similarity of the p_T shape of v_2 between the pPb and PbPb systems provokes the question, whether there is a yet unknown source of v_2 in both systems? In the intermediate region, the anisotropies were found to be larger in minimum-bias than in jet-selected events, and the observed v_2 may come from changing the admixture of particles from

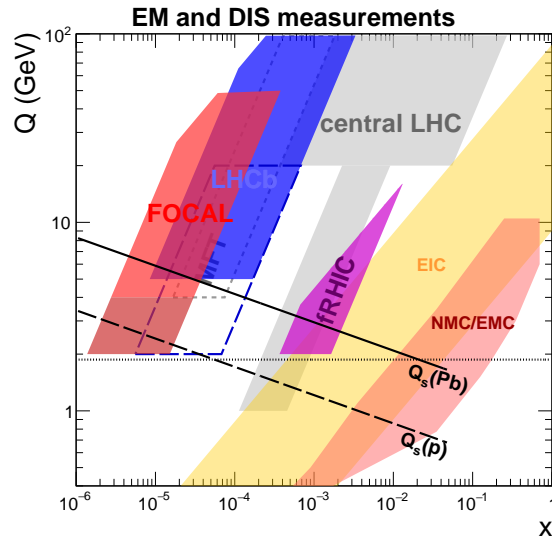


Fig. 3. Approximate (x, Q) coverage of various experiments for regions probed by DIS measurements including at the planned EIC, as well as possible future direct photon and Drell-Yan measurements at RHIC and LHC. The estimated saturation scales for proton and Pb are also indicated. The horizontal dashed line and the dashed curve indicate the kinematic cuts above which data were included in the nNNPDF fits. To calculate x and Q the approximate relations $x = 2p_T / \sqrt{s_{NN}} \exp(-y)$ and $Q = p_T$ was used with $\sqrt{s_{NN}} = 8.8$ TeV for LHC, and $\sqrt{s_{NN}} = 0.2$ TeV for RHIC. Figure from [77].

hard scattering and the underlying event. At $p_T > 10$ GeV/ c , the ATLAS data essentially report long-range correlation between hard and soft particles on the level of 2%, which is remarkably similar to that in PbPb collisions, maybe reflecting some source of residual correlation from the likely presence of a di-jet. It is clear that this question will need to be followed up, maybe by measurements in peripheral PbPb collisions, or by studies using event generators trying to disentangle the various contributions.

Peripheral PbPb collisions, most of the beam energy systems from STAR, as well as small systems (pA and pp collisions) exhibit v_2 but no measurable effect from parton energy loss on the p_T spectra [73–75]. Hence, one of the next key questions is to study the onset of parton energy loss at RHIC and LHC with lighter ions, like for example in OO or ArAr collisions [61]. Unlike in pp or pA collisions, multiplicity distributions in AA collisions exhibit a pronounced plateau that simplifies the centrality determination, and reduces effects from biases induced by the event selection. Indeed, it will be very beneficial to perform the same measurements also at $\sqrt{s_{NN}} = 0.2$ TeV, since the number of MPI per nucleon–nucleon collision will be significantly lower than at LHC energies, while the expected medium properties do not differ greatly. Furthermore, it may be useful to describe the R_{AA} data from the RHIC beam energy scan [74], as well as the SPS data [76] with models including state-of-the-art initial and final state effects.

4. The cold-nuclear matter or small- x frontier

At small longitudinal momentum fraction x and momentum transfer Q , parton dynamics is expected to be affected by non-linear QCD evolution, where the rate of gluon–gluon fusion is in competition with that of gluon splitting. In this kinematic regime, the extremely high gluon density may even saturate, possibly leading to the existence of another pre-collision state of matter – the so-called colour glass condensate (CGC) [78]. The saturation scale, where for a given x the competing processes are in balance, is enhanced in nuclei by a factor $A^{1/3}$ compared to protons, and hence comparisons between measurements in pp and pA collisions are of particular interest.

Figure 3 gives an overview of the approximate (x, Q) coverage of various current and future experiments for EM or DIS measurements. At RHIC and EIC a region down to about $x \sim 10^{-4}$ will be probed with

the future direct photon and Drell-Yan measurements enabled by the RHIC cold nuclear program [79], for which STAR and sPHENIX plan forward upgrades at $2.5 < \eta < 4$ [80, 81]. Shown are also regions probed by nuclear DIS measurements [82–84], including at the planned EIC [85]. Due to the large beam energy available at the LHC, instrumenting the forward region at the LHC enables measurements probing parton densities at small x of the proton or nucleus, down to $x \sim 10^{-6}$, over a large range in Q^2 . The LHCb experiment [86] is a single-arm spectrometer equipped with tracking and particle-identification detectors as well as calorimeters with a forward angular coverage of about $2 < \eta < 5$. The FoCal is high-granularity Si+W electromagnetic calorimeter and metal+scintillator hadron calorimeter at $3.4 < \eta < 5.8$ proposed to be installed in ALICE in LS3 [77]. The FoCal and LHCb measurements probe much smaller x than any of the other experiments. The FoCal will access the smallest x ever measurable until the possible advent of the LHeC [87] or FCC [88]. Compared to RHIC, the LHC will give access to a significantly larger region of phase space that is potentially affected by parton saturation. In particular, the region of gluon saturation will extend to p_T values high enough that perturbative QCD should be applicable.

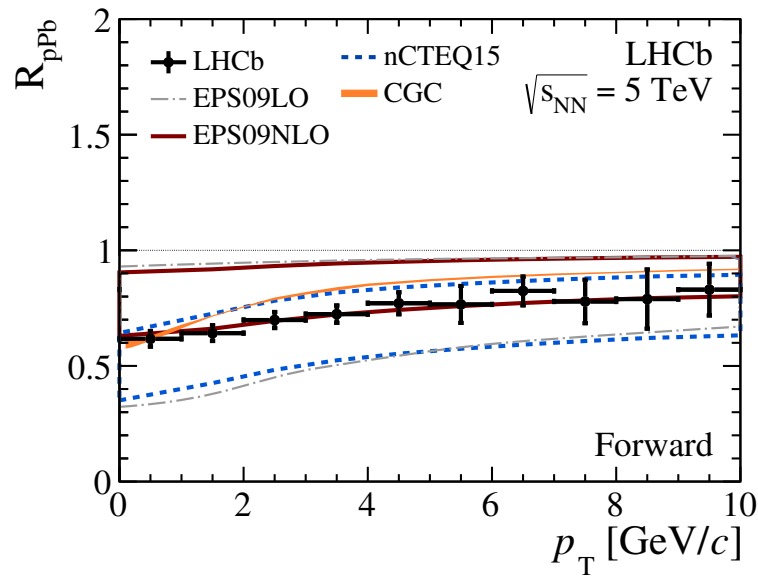


Fig. 4. Nuclear modification factor R_{pPb} as a function of p_T for prompt D^0 integrated over $2.5 < |y^*| < 4.0$ for $p_T < 6$ GeV/c and $2.5 < |y^*| < 3.5$ for $6 < p_T < 10$ GeV/c for pPb collisions at $\sqrt{s_{NN}} = 5.02$ TeV as measured by LHCb compared to theoretical predictions of different pQCD calculations using nuclear PDFs and a recent CGC calculation. The figure is adapted from [89].

Precise information at forward rapidity probing small x at the LHC is provided by the measurement of prompt D-meson production at $2.5 < y < 4.0$ by LHCb [89]. D-meson production is directly sensitive to the gluon density, since the dominant production process for $c\bar{c}$ production is gluon fusion $gg \rightarrow c\bar{c}$. The measured nuclear modification factor R_{pPb} as a function of p_T at forward rapidities (Fig. 4) exhibits that the forward production of prompt D-mesons is suppressed compared to pp collisions, with $R_{pPb} \sim 0.6$ at low p_T and increasing mildly with p_T . The measured suppression is consistent with expectations based on the various calculations using nuclear PDFs or the CGC framework. The suppression of charm production in the calculations with nuclear PDFs is a direct result of the reduced gluon density at $x \lesssim 10^{-2}$, which is commonly referred to as *gluon shadowing*. The calculated values range from R_{pPb} about 0.3 to 0.9, reflecting the current uncertainties in the nuclear modification of the small- x gluon density. This directly confirms that shadowing at small x is large, and that the data place constraints on nuclear PDFs, as discussed at the conference [90].

However, a quantitative determination of the amount of gluon shadowing based on hadron production measurements is complicated by the fact that hadronic final state effects (rescattering) may also play a role in the observations. Recent forward measurements from LHCb at $\sqrt{s_{NN}} = 8.16$ TeV include the observations

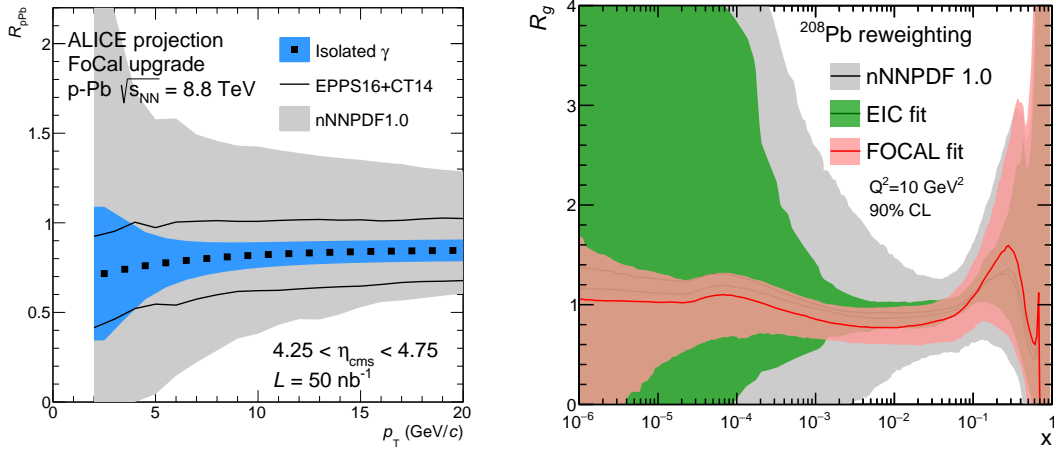


Fig. 5. Left panel: Expected uncertainty for the nuclear modification factor of isolated photons at $\sqrt{s_{NN}} = 8.8$ TeV measured with FoCal. The bands indicate the systematic uncertainty, mostly due to uncertainties on the efficiency and energy scale, as well as the decay photon background determination. The current EPPS16 and nNNPDF1.0 uncertainties are indicated by the black line and the shaded band, respectively. Right panel: The nuclear modification of the gluon distribution for Pb versus x at $Q^2 = 10 \text{ GeV}^2/c^2$ for $x > 10^{-6}$ compared between nNNPDF1.0 parameterization and fits to the FoCal pseudo-data (red band) and “high energy” EIC pseudo-data (green band). 90% confidence-level uncertainty bands are drawn, and the nuclear PDFs are normalized by the proton NNPDF3.1. Figures from [77].

of a stronger suppression of the cross section ratio of $Y(1S)$ to J/ψ from b in pPb compared to pp collisions, as well as stronger nuclear modification of $Y(2S)$ compared to $Y(1S)$ [91]. Both require the presence of additional (final-state) effects to describe the data. Also, the forward/backward ratio of D-meson production at high p_T in pPb collisions at $\sqrt{s_{NN}} = 8.16$ TeV [92] differs from expectation of models and data at 5 TeV.

A clean probe providing direct access to partons are direct photons, since they couple to quarks, and are not affected by final-state nor hadronization effects. At leading-order more than 70% are produced by Compton ($qg \rightarrow \gamma q$) process, hence directly sensitive to the gluon density. An essential design goal of proposed FoCal [77] is ability to reconstruct $\pi^0 \rightarrow \gamma\gamma$ decays at forward rapidity up to large transverse momenta $p_T \sim 20 \text{ GeV}/c$ with high efficiency. This will enable precise discrimination between direct photons and decay photons, hence enabling to measure direct photons from low transverse momentum up to $\sim 20 \text{ GeV}/c$ at large rapidity. The unique performance of a future isolated photon measurement with FoCal is demonstrated in Fig. 5. An accuracy of about 20% is expected at $4 \text{ GeV}/c$, improving to about 5% at $10 \text{ GeV}/c$ and above, which will strongly constrain nuclear PDFs below $x \sim 0.001$, in a region complementary to the EIC.

5. The ultra-precision near and far future

An overview of the timeline of planned and proposed near- and far-future instrumentation for high-energy nuclear physics, grouped into different categories (high density, high energy, small- x and ultra-precision future) is given in Fig. 6. Besides the ongoing experimental program, in particular at RHIC and SPS, new dedicated future experiments and facilities are being built over the next 5–10 years to characterize the phase structure of strongly-interacting matter at high μ_B [93]. In addition, at the LHC, data can be taken in fixed-target mode, for example by LHCb with the SMOG2 system [94], allowing to probe the freeze-out curve up to $\mu_B \approx 400 \text{ MeV}$ (see summary in [95]).

In 2021 the ALICE LS2 upgrades [96, 97] to improve the capabilities for rare probes at low p_T will have been completed, which in particular include a new inner tracking system based on MAPS [98], the GEM-based TPC readout [99], and the forward muon tracker [100]. LHCb, will complete its LS2 upgrades [101], with

among more minor improvements, a new pixel vertex locator [102] and a new high-granularity silicon micro-strip planes upstream and scintillating-fibre downstream tracker [103] usable in up to 30–100% central PbPb collisions. In 2023, sPHENIX [104] is expected to start operating specifically designed for measurements of hard probes at RHIC. The major upgrades for CMS [105] and ATLAS [106] are prepared for data taking in 2027 after LS3. For CMS, they mainly are a new high-granularity pixel and Si-strip tracking system up to $\eta < 3.8$ [107] with a MIP timing layer for time-of-flight measurements [108] and a high-granularity calorimeter [109]. For ATLAS, similarly, they mainly are a new high-granularity pixel and Si-strip tracking system up to $\eta < 4$ [110]. In LS3, the ALICE collaboration will replace the inner-most pixel layers with truly cylindrical layers using thinned, wafer-sized sensors [111], which will further improve the secondary vertex finding as well as tracking efficiency and momentum resolution at low p_T .

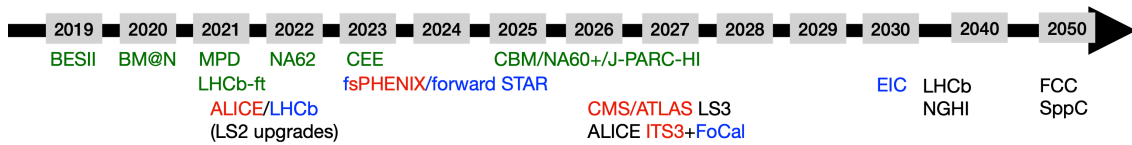


Fig. 6. Timeline of planned and proposed near- and far-future instrumentation for high-energy nuclear physics, grouped into: the high-density frontier (green) with BESII [112], BM@N [113], MPD [114], LHCb fixed-target [94], NA62 [8], CEE [115], CBM [11], NA60+ [9], J-PARK-HI [12]; the high-energy frontier (red) with ALICE LS2 upgrades [96, 97], sPHENIX [104], CMS LS3 upgrades [105] and ATLAS LS3 upgrades [106], ALICE ITS3 [111]; the small- x frontier (blue) with LHCb phase-1 upgrade [101], forward sPHENIX [80], forward STAR [81], FoCal [77], EIC [85]; the ultra-precision future (black): LHCb phase-2 upgrade [116], NGHI [117], FCC [5], SppS [118].

Besides the LHCb after its phase-1 upgrade [101], the proposed forward upgrades [80, 81] at RHIC and FoCal [77] at the LHC, there is the planned EIC [85] expected to begin data-taking around 2030. The EIC will be ep and eA polarized (up to small nuclei) collider dedicated to the study of proton and nuclei structures. The collider will enable DIS off a proton or a nucleus with a range of $20 < \sqrt{s} < 140$ GeV and a luminosity of $10^{34} \text{ cm}^{-2}\text{s}^{-1}$. It will allow us to systematically explore correlations inside protons and nuclei, as well as to study saturation and hadronization with a controllable initial state. For an overview of the EIC physics program and the connection to heavy-ion physics, given at the conference, see [119].

For data-taking at similar timescale as the EIC, the successor of ALICE, the Next Generation Heavy Ion (NGHI) has been proposed [117]. It is designed as a fast, ultra-thin detector with precise tracking and timing, and will provide the ultimate performance for measurements related to (multi-)heavy-flavor, soft hadrons and thermal radiation over large range in rapidity $\eta \leq 4$. Eventually one can add far-forward tracking and particle identification capabilities to access the high net-baryons and/or a far forward calorimeter for ultra-soft- x photons. In 2030, LHCb will also have concluded its phase-2 upgrade [116], after which its tracking detectors will be able to cope with even higher track densities of the HL-LHC. This will also allow the reconstruction of central PbPb data, and open up the full suite of particle identification provided by the LHCb spectrometer at forward rapidity inPbPb collisions. Together with ATLAS and CMS, these experiments will provide an incredibly rich, precision high-density QCD and heavy-ion program at the LHC, in parallel to the precision cold nuclear matter program the EIC. As indicated also in Fig. 6, the far-future perspective is equally bright, given the activities related to the FCC [5] including preparations for a heavy-ion program [120] and the CEPC-SppC [118].

6. Summary

Instead of a “summary of the summary”, let me just point out that —without any doubt— we are experiencing the golden age of high-density QCD and heavy-ion physics, with a numerous interesting problems to solve and an extremely bright future in instrumentation ahead.

Acknowledgements

I would like to thank the conference organizers for their endless effort to create such a stimulating and successful conference, and for being so extra-ordinary hosts. Support by the U.S. Department of Energy, Office of Science, Office of Nuclear Physics, under contract number DE-AC05-00OR22725, is greatly appreciated.

References

- [1] W. Busza, K. Rajagopal, W. van der Schee, Heavy-ion collisions: The big picture, and the big questions, *Ann. Rev. Nucl. Part. Sci.* 68 (2018) 339–376. [arXiv:1802.04801](#).
- [2] H.-T. Ding, New developments in lattice QCD on equilibrium physics and phase diagram, in: 28th International Conference on Ultrarelativistic Nucleus-Nucleus Collisions, 2020. [arXiv:2002.11957](#).
- [3] C. Loizides, “Summary” talk: Outlook and future of heavy-ion physics, talk given at QM19.
- [4] LHC Machine, JINST 3 (2008) S08001. [doi:10.1088/1748-0221/3/08/S08001](#).
- [5] M. Benedikt, A. Blondel, P. Janot, M. Mangano, F. Zimmermann, Future Circular Colliders succeeding the LHC, *Nature Phys.* 16 (4) (2020) 402–407. [doi:10.1038/s41567-020-0856-2](#).
- [6] M. Harrison, T. Ludlam, S. Ozaki, RHIC project overview, *Nucl. Instrum. Meth. A* 499 (2003) 235–244. [doi:10.1016/S0168-9002\(02\)01937-X](#).
- [7] M. Aggarwal, et al., An experimental exploration of the QCD phase diagram: The Search for the Critical Point and the onset of de-confinement [arXiv:1007.2613](#).
- [8] A. Aduszkiewicz, Study of hadron–nucleus and nucleus–nucleus collisions at the CERN SPS: Early post-LS2 measurements and future plans, Tech. Rep. CERN-SPSC-2018-008. SPSC-P-330-ADD-10, CERN, Geneva (Mar 2018). URL <https://cds.cern.ch/record/2309890>
- [9] T. Dahms, E. Scomparin, G. Usai, Expression of Interest for a new experiment at the CERN SPS: NA60+, Tech. Rep. CERN-SPSC-2019-017. SPSC-EOI-019, CERN, Geneva (May 2019). URL <http://cds.cern.ch/record/2673280>
- [10] V. Kekelidze, V. Matveev, I. Meshkov, A. Sorin, G. Trubnikov, Project Nuclotron-based Ion Collider fAcility at JINR, *Phys. Part. Nucl.* 48 (5) (2017) 727–741. [doi:10.1134/S1063779617050239](#).
- [11] P. Senger, Probing dense QCD matter in the laboratory: The CBM experiment at FAIR [arXiv:2005.03321](#), [doi:10.1088/1402-4896/ab8c14](#).
- [12] H. Sako, Future Heavy-Ion Program at J-PARC, *JPS Conf. Proc.* 8 (2015) 022010. [doi:10.7566/JPSCP.8.022010](#).
- [13] A. Dainese, Future facilities and experiments, talk given at QM19.
- [14] S. Borsanyi, Z. Fodor, J. N. Guenther, R. Kara, S. D. Katz, P. Parotto, A. Pasztor, C. Ratti, K. K. Szabo, The QCD crossover at finite chemical potential from lattice simulations [arXiv:2002.02821](#).
- [15] A. Bzdak, S. Esumi, V. Koch, J. Liao, M. Stephanov, N. Xu, Mapping the phases of Quantum Chromodynamics with Beam Energy Scan, *Phys. Rept.* 853 (2020) 1–87. [arXiv:1906.00936](#), [doi:10.1016/j.physrep.2020.01.005](#).
- [16] A. Andronic, P. Braun-Munzinger, K. Redlich, J. Stachel, Decoding the phase structure of QCD via particle production at high energy, *Nature* 561 (7723) (2018) 321–330. [arXiv:1710.09425](#), [doi:10.1038/s41586-018-0491-6](#).
- [17] T. Nonaka, Measurement of the sixth-order cumulant of net-proton distributions in AuAu collisions from the STAR experiment, in: 28th International Conference on Ultrarelativistic Nucleus-Nucleus Collisions, 2020. [arXiv:2002.12505](#).
- [18] B. Friman, F. Karsch, K. Redlich, V. Skokov, Fluctuations as probe of the QCD phase transition and freeze-out in heavy ion collisions at LHC and RHIC, *Eur. Phys. J. C* 71 (2011) 1694. [arXiv:1103.3511](#), [doi:10.1140/epjc/s10052-011-1694-2](#).
- [19] S. Gupta, D. Mallick, D. K. Mishra, B. Mohanty, N. Xu, Freeze-out and thermalization in relativistic heavy ion collisions [arXiv:2004.04681](#).
- [20] K. Nayak, Directed and elliptic flow of identified hadrons, high- p_T charged hadrons and light nuclei in AuAu collisions at STAR, in: 28th International Conference on Ultrarelativistic Nucleus-Nucleus Collisions, 2020. [arXiv:2002.12066](#).
- [21] H. Stoecker, Collective flow signals the quark gluon plasma, *Nucl. Phys. A* 750 (2005) 121–147. [arXiv:nuc1-th/0406018](#), [doi:10.1016/j.nuclphysa.2004.12.074](#).
- [22] S. Mukherjee, V. Koch, et al., Beam Energy Scan Theory Collaboration, <https://www.bnl.gov/physics/best/> (2020).
- [23] C. Shen, Studying QGP with flow: A theory overview, in: 28th International Conference on Ultrarelativistic Nucleus-Nucleus Collisions, 2020. [arXiv:2001.11858](#).
- [24] P. Parotto, M. Bluhm, D. Mroczek, M. Nahrgang, J. Noronha-Hostler, K. Rajagopal, C. Ratti, T. Schfer, M. Stephanov, QCD equation of state matched to lattice data and exhibiting a critical point singularity, *Phys. Rev. C* 101 (3) (2020) 034901. [arXiv:1805.05249](#), [doi:10.1103/PhysRevC.101.034901](#).
- [25] G. Aad, et al., Longitudinal flow decorrelations in XeXe collisions at $\sqrt{s_{NN}} = 5.44$ TeV with the ATLAS detector [arXiv:2001.04201](#).
- [26] M. Nie, Energy dependence of longitudinal flow decorrelation from STAR [arXiv:2005.03252](#).
- [27] S. Acharya, et al., Non-linear flow modes of identified particles in PbPb collisions at $\sqrt{s_{NN}} = 5.02$ TeV [arXiv:1912.00740](#).
- [28] Y. Zhu, Anisotropic flow fluctuations of charged and identified hadrons in PbPb collisions with the ALICE detector, in: 28th International Conference on Ultrarelativistic Nucleus-Nucleus Collisions, 2020. [arXiv:todo](#).
- [29] J. Putschke, et al., The JETSCAPE framework [arXiv:1903.07706](#).

- [30] J.-F. Paquet, et al., Revisiting Bayesian constraints on the transport coefficients of QCD, in: 28th International Conference on Ultrarelativistic Nucleus-Nucleus Collisions, 2020. [arXiv:2002.05337](#).
- [31] X. Bai, Quarkonium measurements in nucleus-nucleus collisions with ALICE, in: 28th International Conference on Ultrarelativistic Nucleus-Nucleus Collisions, 2020. [arXiv:todo](#).
- [32] M. Gazdzicki, M. I. Gorenstein, Evidence for statistical production of J/ψ mesons in nuclear collisions at the CERN SPS, *Phys. Rev. Lett.* 83 (1999) 4009–4012. [arXiv:hep-ph/9905515](#), doi:10.1103/PhysRevLett.83.4009.
- [33] R. L. Thews, M. Schroedter, J. Rafelski, Enhanced J/ψ production in deconfined quark matter, *Phys. Rev. C* 63 (2001) 054905. [arXiv:hep-ph/0007323](#), doi:10.1103/PhysRevC.63.054905.
- [34] A. Andronic, P. Braun-Munzinger, K. Redlich, J. Stachel, Statistical hadronization of charm in heavy ion collisions at SPS, RHIC and LHC, *Phys. Lett. B* 571 (2003) 36–44. [arXiv:nucl-th/0303036](#), doi:10.1016/j.physletb.2003.07.066.
- [35] S. Acharya, et al., J/ψ elliptic and triangular flow in PbPb collisions at $\sqrt{s_{NN}}=5.02$ TeV [arXiv:2005.14518](#).
- [36] G. M. Innocenti, Latest results on Λ_c^+ and D production in pp and PbPb collisions at $\sqrt{s_{NN}} = 5.02$ TeV with ALICE at the LHC, in: 28th International Conference on Ultrarelativistic Nucleus-Nucleus Collisions, 2020. [arXiv:todo](#).
- [37] R. Larsen, S. Meinel, S. Mukherjee, P. Petreczky, Excited bottomonia in quark-gluon plasma from lattice QCD, *Phys. Lett. B* 800 (2020) 135119. [arXiv:1910.07374](#), doi:10.1016/j.physletb.2019.135119.
- [38] A. M. Sirunyan, et al., Measurement of the azimuthal anisotropy of $\Upsilon(1S)$ and $\Upsilon(2S)$ mesons in PbPb collisions at $\sqrt{s_{NN}}=5.02$ TeV [arXiv:2006.07707](#).
- [39] Measurement of the elliptic flow of $\Upsilon(1S)$ and $\Upsilon(2S)$ mesons in PbPb collisions at $\sqrt{s_{NN}} = 5.02$ TeV, Tech. Rep. CMS-PAS-HIN-19-002, CERN, Geneva (2019).
URL <https://cds.cern.ch/record/2698580>
- [40] S. Acharya, et al., Measurement of $\Upsilon(1S)$ elliptic flow at forward rapidity in PbPb collisions at $\sqrt{s_{NN}} = 5.02$ TeV, *Phys. Rev. Lett.* 123 (19) (2019) 192301. [arXiv:1907.03169](#), doi:10.1103/PhysRevLett.123.192301.
- [41] K. Reygers, A. Schmah, A. Berdnikova, X. Sun, Blast-wave description of Upsilon elliptic flow at LHC energies [arXiv:1910.14618](#).
- [42] A. M. Sirunyan, et al., Observation of medium-induced modifications of jet fragmentation in PbPb collisions at $\sqrt{s_{NN}}=5.02$ TeV using isolated photon-tagged jets, *Phys. Rev. Lett.* 121 (24) (2018) 242301. [arXiv:1801.04895](#), doi:10.1103/PhysRevLett.121.242301.
- [43] N. Borghini, U. A. Wiedemann, Distorting the hump-backed plateau of jets with dense QCD matter [arXiv:hep-ph/0506218](#).
- [44] Studies of parton-medium interactions using Z-tagged charged particles in PbPb collisions at $\sqrt{s_{NN}} = 5.02$ TeV, Tech. Rep. CMS-PAS-HIN-19-006, CERN, Geneva (2020).
URL <https://cds.cern.ch/record/2718841>
- [45] M. Aaboud, et al., Measurement of the nuclear modification factor for inclusive jets in PbPb collisions at $\sqrt{s_{NN}} = 5.02$ TeV with the ATLAS detector, *Phys. Lett. B* 790 (2019) 108–128. [arXiv:1805.05635](#), doi:10.1016/j.physletb.2018.10.076.
- [46] S. Acharya, et al., Measurements of inclusive jet spectra in pp and central Pb-Pb collisions at $\sqrt{s_{NN}} = 5.02$ TeV, *Phys. Rev. C* 101 (3) (2020) 034911. [arXiv:1909.09718](#), doi:10.1103/PhysRevC.101.034911.
- [47] Measurement of jet nuclear modification factor in PbPb collisions at $\sqrt{s_{NN}} = 5.02$ TeV with CMS.
- [48] C. Loizides, A. Morsch, Absence of jet quenching in peripheral nucleus-nucleus collisions, *Phys. Lett. B* 773 (2017) 408–411. [arXiv:1705.08856](#), doi:10.1016/j.physletb.2017.09.002.
- [49] V. Khachatryan, et al., Charged-particle nuclear modification factors in PbPb and pPb collisions at $\sqrt{s_{NN}} = 5.02$ TeV, *JHEP* 04 (2017) 039. [arXiv:1611.01664](#), doi:10.1007/JHEP04(2017)039.
- [50] R. Haake, C. Loizides, Machine Learning based jet momentum reconstruction in heavy-ion collisions, *Phys. Rev. C* 99 (6) (2019) 064904. [arXiv:1810.06324](#), doi:10.1103/PhysRevC.99.064904.
- [51] R. Haake, Machine Learning based jet momentum reconstruction in PbPb collisions measured with the ALICE detector, in: 2019 European Physical Society Conference on High Energy Physics, 2019. [arXiv:1909.01639](#).
- [52] S. Marzani, G. Soyez, M. Spannowsky, Looking inside jets: an introduction to jet substructure and boosted-object phenomenology, Vol. 958, Springer, 2019. [arXiv:1901.10342](#), doi:10.1007/978-3-030-15709-8.
- [53] L. Havener, Jet splitting measurements in PbPb and pp collisions at $\sqrt{s_{NN}} = 5.02$ TeV with ALICE, in: 28th International Conference on Ultrarelativistic Nucleus-Nucleus Collisions, 2020. [arXiv:2002.05307](#).
- [54] Measurement of suppression of large-radius jets and its dependence on substructure in PbPb at 5.02 TeV by ATLAS detector, Tech. Rep. ATLAS-CONF-2019-056, CERN, Geneva (Nov 2019).
URL <https://cds.cern.ch/record/2701506>
- [55] J. L. Nagle, W. A. Zajc, Small system collectivity in relativistic hadronic and nuclear collisions, *Ann. Rev. Nucl. Part. Sci.* 68 (2018) 211–235. [arXiv:1801.03477](#), doi:10.1146/annurev-nucl-101916-123209.
- [56] S. Pisano, Light-flavour hadron production vs. multiplicity in pp and in pPb collisions with ALICE, in: 28th International Conference on Ultrarelativistic Nucleus-Nucleus Collisions, 2020.
- [57] V. Vislavicius, A. Kalweit, Multiplicity dependence of light flavour hadron production at LHC energies in the strangeness canonical suppression picture [arXiv:1610.03001](#).
- [58] C. Loizides, Experimental overview on small collision systems at the LHC, *Nucl. Phys. A* 956 (2016) 200–207. [arXiv:1602.09138](#).
- [59] Y. Kanakubo, Y. Tachibana, T. Hirano, Unified description of hadron yield ratios from dynamical core-corona initialization, *Phys. Rev. C* 101 (2) (2020) 024912. [arXiv:1910.10556](#), doi:10.1103/PhysRevC.101.024912.
- [60] J. Adolfsson, et al., QCD Challenges from pp to AA collisions, 2020. [arXiv:2003.10997](#).
- [61] Z. Citron, et al., Report from Working Group 5: Future physics opportunities for high-density QCD at the LHC with heavy-ion and proton beams, Vol. 7, 2019, pp. 1159–1410. [arXiv:1812.06772](#), doi:10.23731/CYRM-2019-007.1159.
- [62] Studies of charm and beauty long-range correlations in pp and pPb collisions, Tech. Rep. CMS-PAS-HIN-19-009, CERN,

- Geneva (2019).
URL <https://cds.cern.ch/record/2699456>
- [63] G. Aad, et al., Measurement of azimuthal anisotropy of muons from charm and bottom hadrons in pp collisions at $\sqrt{s} = 13$ TeV with the ATLAS detector, Phys. Rev. Lett. 124 (8) (2020) 082301. arXiv:1909.01650, doi:10.1103/PhysRevLett.124.082301.
- [64] C. Aidala, et al., Creation of quark–gluon plasma droplets with three distinct geometries, Nature Phys. 15 (3) (2019) 214–220. arXiv:1805.02973, doi:10.1038/s41567-018-0360-0.
- [65] M. Aaboud, et al., Measurement of long-range two-particle azimuthal correlations in Z-boson tagged pp collisions at $\sqrt{s}=8$ and 13 TeV, Eur. Phys. J. C 80 (1) (2020) 64. arXiv:1906.08290, doi:10.1140/epjc/s10052-020-7606-6.
- [66] Two-particle azimuthal correlations in photo-nuclear ultra-peripheral PbPb collisions at 5.02 TeV with ATLAS, Tech. Rep. ATLAS-CONF-2019-022, CERN, Geneva (Jun 2019).
URL <https://cds.cern.ch/record/2679473>
- [67] A. Badea, A. Baty, P. Chang, G. M. Innocenti, M. Maggi, C. McGinn, M. Peters, T.-A. Sheng, J. Thaler, Y.-J. Lee, Measurements of two-particle correlations in e^+e^- collisions at 91 GeV with ALEPH archived data, Phys. Rev. Lett. 123 (21) (2019) 212002. arXiv:1906.00489, doi:10.1103/PhysRevLett.123.212002.
- [68] I. Abt, et al., Two-particle azimuthal correlations as a probe of collective behaviour in deep inelastic ep scattering at HERA, JHEP 04 (2020) 070. arXiv:1912.07431, doi:10.1007/JHEP04(2020)070.
- [69] B. Schenke, C. Shen, P. Tribedy, Hybrid Color Glass Condensate and hydrodynamic description of the Relativistic Heavy Ion Collider small system scan, Phys. Lett. B 803 (2020) 135322. arXiv:1908.06212, doi:10.1016/j.physletb.2020.135322.
- [70] J. Adam, et al., Centrality dependence of particle production in p-Pb collisions at $\sqrt{s_{NN}}=5.02$ TeV, Phys. Rev. C 91 (6) (2015) 064905. arXiv:1412.6828, doi:10.1103/PhysRevC.91.064905.
- [71] A. Sirunyan, et al., Azimuthal anisotropy of charged particles with transverse momentum up to 100 GeV/c in PbPb collisions at $\sqrt{s_{NN}}=5.02$ TeV, Phys. Lett. B 776 (2018) 195–216. arXiv:1702.00630, doi:10.1016/j.physletb.2017.11.041.
- [72] G. Aad, et al., Transverse momentum and process dependent azimuthal anisotropies in $\sqrt{s_{NN}} = 8.16$ TeV pPb collisions with the ATLAS detector, Eur. Phys. J. C 80 (1) (2020) 73. arXiv:1910.13978, doi:10.1140/epjc/s10052-020-7624-4.
- [73] S. Acharya, et al., Analysis of the apparent nuclear modification in peripheral Pb–Pb collisions at 5.02 TeV, Phys. Lett. B 793 (2019) 420–432. arXiv:1805.05212, doi:10.1016/j.physletb.2019.04.047.
- [74] L. Adamczyk, et al., Beam energy dependence of jet-quenching effects in AuAu collisions at $\sqrt{s_{NN}} = 7.7, 11.5, 14.5, 19.6, 27, 39,$ and 62.4 GeV, Phys. Rev. Lett. 121 (3) (2018) 032301. arXiv:1707.01988, doi:10.1103/PhysRevLett.121.032301.
- [75] L. Adamczyk, et al., Elliptic flow of identified hadrons in AuAu collisions at $\sqrt{s_{NN}} = 7.7-62.4$ GeV, Phys. Rev. C 88 (2013) 014902. arXiv:1301.2348, doi:10.1103/PhysRevC.88.014902.
- [76] C. Alt, et al., High transverse momentum hadron spectra at $\sqrt{s_{NN}} = 17.3$ GeV in PbPb and pp collisions measured by CERN-NA49, Phys. Rev. C 77 (2008) 034906. arXiv:0711.0547, doi:10.1103/PhysRevC.77.034906.
- [77] A. Collaboration, Letter of Intent: A Forward Calorimeter (FoCal) in the ALICE experiment, Tech. Rep. CERN-LHCC-2020-009. LHCC-I-036, CERN, Geneva (Jun 2020).
URL <https://cds.cern.ch/record/2719928>
- [78] F. Gelis, Color Glass Condensate and Glasma, Int. J. Mod. Phys. A28 (2013) 1330001. arXiv:1211.3327, doi:10.1142/S0217751X13300019.
- [79] E.-C. Aschenauer, et al., The RHIC Cold QCD Plan for 2017 to 2023: A Portal to the EIC arXiv:1602.03922.
- [80] sPHENIX Forward Instrumentation - A letter of intent, sPHENIX-note sPH-cQCD-2017-001.
- [81] The STAR forward calorimeter system and forward tracking system, ForwardUpgrade.v20.
- [82] M. Arneodo, et al., The structure function ratios $F_2^{\text{Li}}/F_2^{\text{d}}$ and $F_2^{\text{C}}/F_2^{\text{d}}$ at small x , Nucl. Phys. B441 (1995) 12–30. arXiv:hep-ex/9504002, doi:10.1016/0550-3213(95)00023-2.
- [83] M. Arneodo, et al., Measurement of the proton and the deuteron structure functions, F_2^{p} and F_2^{d} , Phys. Lett. B364 (1995) 107–115. arXiv:hep-ph/9509406, doi:10.1016/0370-2693(95)01318-9.
- [84] M. Arneodo, et al., The Q^2 dependence of the structure function ratio $F_2^{\text{Sn}}/F_2^{\text{C}}$ and the difference $R^{\text{Sn}} - R^{\text{C}}$ in deep inelastic muon scattering, Nucl. Phys. B481 (1996) 23–39. doi:10.1016/S0550-3213(96)90119-4.
- [85] A. Accardi, et al., Electron Ion Collider: The next QCD frontier, Eur. Phys. J. A52 (9) (2016) 268. arXiv:1212.1701, doi:10.1140/epja/i2016-16268-9.
- [86] J. Alves, et al., The LHCb Detector at the LHC, JINST 3 (2008) S08005. doi:10.1088/1748-0221/3/08/S08005.
- [87] J. L. Abelleira Fernandez, et al., A Large Hadron Electron Collider at CERN: Report on the physics and design concepts for machine and detector, J. Phys. G39 (2012) 075001. arXiv:1206.2913, doi:10.1088/0954-3899/39/7/075001.
- [88] A. Abada, et al., Future Circular Collider: Physics opportunities, CERN-ACC-2018-0056.
- [89] R. Aaij, et al., Study of prompt D^0 meson production in pPb collisions at $\sqrt{s_{NN}} = 5$ TeV, JHEP 10 (2017) 090. arXiv:1707.02750, doi:10.1007/JHEP10(2017)090.
- [90] K. J. Eskola, I. Helenius, P. Paakkinen, H. Paukkunen, Impact of dijet and D-meson data from 5.02 TeV pPb collisions on nuclear PDFs, in: 28th International Conference on Ultrarelativistic Nucleus-Nucleus Collisions, 2020. arXiv:2001.10385.
- [91] R. Aaij, et al., Study of Υ production in pPb collisions at $\sqrt{s_{NN}} = 8.16$ TeV, JHEP 11 (2018) 194, [Erratum: JHEP 02, 093 (2020)]. arXiv:1810.07655, doi:10.1007/JHEP11(2018)194.
- [92] R. Aaij, et al., Study of prompt D^0 meson production in pPb at $\sqrt{s_{NN}} = 8.16$ TeV at LHCb, Tech. Rep. LHCb-CONF-2019-004 (Nov 2019).
URL <https://cds.cern.ch/record/2700244>
- [93] T. Galatyuk, Future facilities for high μ_B physics, Nucl. Phys. A 982 (2019) 163–169. doi:10.1016/j.nuclphysa.2018.11.025.

- [94] L. Collaboration, LHCb SMOG Upgrade, Tech. Rep. CERN-LHCC-2019-005. LHCb-TDR-020, CERN, Geneva (May 2019). URL <https://cds.cern.ch/record/2673690>
- [95] V. Begun, D. Kikoř a, V. Vovchenko, D. Wielanek, Estimation of the freeze-out parameters reachable in a fixed-target experiment at the CERN Large Hadron Collider, Phys. Rev. C 98 (3) (2018) 034905. [arXiv:1806.01303](https://arxiv.org/abs/1806.01303), doi:10.1103/PhysRevC.98.034905.
- [96] B. Abelev, et al., Upgrade of the ALICE Experiment: Letter Of Intent, J. Phys. G 41 (2014) 087001. doi:10.1088/0954-3899/41/8/087001.
- [97] B. Abelev, et al., Addendum of the Letter of Intent for the upgrade of the ALICE experiment : The Muon Forward Tracker, Tech. Rep. CERN-LHCC-2013-014. LHCC-I-022-ADD-1, CERN, Geneva (Aug 2013). URL <https://cds.cern.ch/record/1592659>
- [98] B. Abelev, et al., Technical Design Report for the Upgrade of the ALICE Inner Tracking System, Tech. Rep. CERN-LHCC-2013-024. ALICE-TDR-017 (Nov 2013). doi:10.1088/0954-3899/41/8/087002. URL <https://cds.cern.ch/record/1625842>
- [99] C. Lippmann, et al., Upgrade of the ALICE Time Projection Chamber, Tech. Rep. CERN-LHCC-2013-020. ALICE-TDR-016 (Oct 2013). URL <https://cds.cern.ch/record/1622286>
- [100] B. Abelev, et al., Technical Design Report for the Muon Forward Tracker, Tech. Rep. CERN-LHCC-2015-001. ALICE-TDR-018 (Jan 2015). URL <https://cds.cern.ch/record/1981898>
- [101] LHCb, LHCb projections for proton-lead collisions during LHC Runs 3 and 4, CERN, CERN, Geneva, 2018.
- [102] C. Paula, R. Lindner, et al., LHCb VELO Upgrade Technical Design Report, Tech. Rep. CERN-LHCC-2013-021. LHCb-TDR-013 (Nov 2013). URL <https://cds.cern.ch/record/1624070>
- [103] M. Ferro-luzzi, R. Lindner, et al., LHCb Tracker Upgrade Technical Design Report, Tech. Rep. CERN-LHCC-2014-001. LHCb-TDR-015 (Feb 2014). URL <https://cds.cern.ch/record/1647400>
- [104] C. Aidala, et al., sPHENIX: An upgrade concept from the PHENIX Collaboration [arXiv:1207.6378](https://arxiv.org/abs/1207.6378).
- [105] J. Butler, D. Contardo, M. Klute, J. Mans, L. Silvestris, et al., CMS Phase II Upgrade Scope Document, Tech. Rep. CERN-LHCC-2015-019. LHCC-G-165, CERN, Geneva (Sep 2015). URL <https://cds.cern.ch/record/2055167>
- [106] K. Einsweiler, L. Pontecorvo, et al., ATLAS Phase-II Upgrade Scoping Document, Tech. Rep. CERN-LHCC-2015-020. LHCC-G-166, CERN, Geneva (Sep 2015). URL <https://cds.cern.ch/record/2055248>
- [107] D. Contardo, A. Ball, et al., The phase-2 upgrade of the CMS tracker, Tech. Rep. CERN-LHCC-2017-009. CMS-TDR-014, CERN, Geneva (Jun 2017). URL <https://cds.cern.ch/record/2272264>
- [108] D. Contardo, A. Ball, et al., A MIP Timing Detector for the CMS Phase-2 Upgrade, Tech. Rep. CERN-LHCC-2019-003. CMS-TDR-020, CERN, Geneva (Mar 2019). URL <https://cds.cern.ch/record/2667167>
- [109] D. Contardo, A. Ball, et al., The Phase-2 Upgrade of the CMS Endcap Calorimeter, Tech. Rep. CERN-LHCC-2017-023. CMS-TDR-019, CERN, Geneva, technical Design Report of the endcap calorimeter for the Phase-2 upgrade of the CMS experiment, in view of the HL-LHC run. (Nov 2017). URL <https://cds.cern.ch/record/2293646>
- [110] K. Einsweiler, L. Pontecorvo, et al., Technical Design Report for the ATLAS Inner Tracker Pixel Detector, Tech. Rep. CERN-LHCC-2017-021. ATLAS-TDR-030, CERN, Geneva (Sep 2017). URL <https://cds.cern.ch/record/2285585>
- [111] L. Musa, et al., Letter of Intent for an ALICE ITS Upgrade in LS3, Tech. Rep. CERN-LHCC-2019-018. LHCC-I-034, CERN, Geneva (Dec 2019). URL <https://cds.cern.ch/record/2703140>
- [112] G. Odyniec, Beam Energy Scan Program at RHIC (BES I and BES II) – Probing QCD phase diagram with heavy-ion collisions, PoS CORFU2018 (2019) 151. doi:10.22323/1.347.0151.
- [113] M. Kapishin, Studies of baryonic matter at the BM@N experiment (JINR), Nucl. Phys. A 982 (2019) 967–970. doi:10.1016/j.nuclphysa.2018.07.014.
- [114] V. Golovatyuk, V. Kekelidze, V. Kolesnikov, O. Rogachevsky, A. Sorin, The Multi-Purpose Detector (MPD) of the collider experiment, Eur. Phys. J. A 52 (8) (2016) 212. doi:10.1140/epja/i2016-16212-1.
- [115] L. L. Yi, Z. Xiao, M. Shao, S. Zhang, G. Xiao, N. Xu, Conceptual design of the HIRFL-CSR external-target experiment, Sci. China Phys. Mech. Astron. 60 (1) (2017) 012021. doi:10.1007/s11433-016-0342-x.
- [116] R. Aaij, et al., Physics case for an LHCb Upgrade II - Opportunities in flavour physics, and beyond, in the HL-LHC era, Tech. Rep. LHCb-PUB-2018-009. LHCC-G-171, CERN, Geneva, ISBN 978-92-9083-494-6 (Aug 2018). URL <https://cds.cern.ch/record/2636441>
- [117] D. Adamov, et al., A next-generation LHC heavy-ion experiment [arXiv:1902.01211](https://arxiv.org/abs/1902.01211).
- [118] M. Ahmad, et al., CEPC-SPPC Preliminary Conceptual Design Report. 1. Physics and Detector.
- [119] Y. Hatta, How EIC can help us to understand heavy-ion collisions, in: 28th International Conference on Ultrarelativistic Nucleus-Nucleus Collisions, 2020. [arXiv:2004.05336](https://arxiv.org/abs/2004.05336).
- [120] A. Dainese, et al., Heavy ions at the Future Circular Collider, CERN Yellow Rep. (3) (2017) 635–692. [arXiv:1605.01389](https://arxiv.org/abs/1605.01389).